Journal: Neurosurgery
Article doi: 10.1093/neuros/nyy152
Article title: Proximal Parent Vessel Tapering is Associated With Aneurysm at the Middle Cerebral Artery Bifurcation
First Author: Alexandra Lauric
Corr. Author: Adel M. Malek

OXFORD JOURNALS
OXFORD UNIVERSITY PRESS

INSTRUCTIONS

We encourage you to use Adobe's editing tools (please see the next page for instructions). If this is not possible, please list clearly in an e-mail. Please do not send corrections as track changed Word documents.

Changes should be corrections of typographical errors only. Changes that contradict journal style will not be made.

These proofs are for checking purposes only. They should not be considered as final publication format. The proof must not be used for any other purpose. In particular we request that you: do not post them on your personal/institutional web site, and do not print and distribute multiple copies. Neither excerpts nor all of the article should be included in other publications written or edited by yourself until the final version has been published and the full citation details are available. You will be sent these when the article is published.

1. **Licence to Publish:** Oxford Journals requires your agreement before publishing your article. If you haven't already completed this, please sign in with your My Account information and complete the online licence form. Details on how to do this can be found in the Welcome to Oxford Journals email.
2. **Permissions: Permission to reproduce any third party material in your paper should have been obtained prior to acceptance. If your paper contains figures or text that require permission to reproduce, please inform me immediately by email.**
3. **Author groups:** Please check that all names have been spelled correctly and appear in the correct order. Please also check that all initials are present. Please check that the author surnames (family name) have been correctly identified by a pink background. If this is incorrect, please identify the full surname of the relevant authors. Occasionally, the distinction between surnames and forenames can be ambiguous, and this is to ensure that the authors' full surnames and forenames are tagged correctly, for accurate indexing online.
4. **Figures:** If applicable, figures have been placed as close as possible to their first citation. Please check that they are complete and that the correct figure legend is present. Figures in the proof are low resolution versions that will be replaced with high resolution versions when the journal is printed.
5. **Missing elements:** Please check that the text is complete and that all figures, tables and their legends are included.
6. **Special characters and equations:** Please check that special characters, equations and units have been reproduced accurately.
7. **URLs:** Please check that all web addresses cited in the text, footnotes and reference list are up-to-date.
8. **Funding:** If applicable, any funding used while completing this work should be highlighted in the Acknowledgements section. Please ensure that you use the full official name of the funding body.

AUTHOR QUERIES - TO BE ANSWERED BY THE CORRESPONDING AUTHOR

The following queries have arisen during the typesetting of your manuscript. Please answer these queries by marking the required corrections at the appropriate point in the text.

Query No.	Nature of Query	Author's Response
Q1	Author: Please confirm that author names are spelled correctly, that author last names are appropriately identified, and that degrees and affiliations for all authors are correct.	Author names, degrees and affiliations are correct for all authors.
Q2	Author: Please provide degree for Alexei Antonov and Gabriel Dardik.	Alexei Antonov and Gabriel Dardik are high school diploma graduates (HSDG).
Q3	Author: Please check table footnotes as set.	Table 1, remove parentheses as indicated in text. Table 2 is correct.
Q4	Author: Please check whether the edit made in the sentence 'In addition, some controls also displayed…' retains the intended sense.	This is correct.
Q5	Author: Please check whether reference (8) is okay as set.	This is correct.
Q6	Author: Please provide complete page range for reference 21.	*Surg Neurol Int*. is an online only continuous publication journal. No page range available
Q7	Author: Please note that issue number is unavailable for reference 21.	See above. Correct reference: *Surg Neurol Int*. 2011;2:35. doi:10.4103/2152-7806.78243.

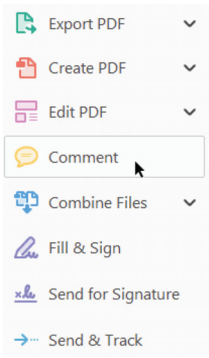
MAKING CORRECTIONS TO YOUR PROOF

These instructions show you how to mark changes or add notes to your proofs using Adobe Acrobat Professional versions 7 and onwards, or Adobe Reader DC. To check what version you are using go to **Help** then **About**. The latest version of Adobe Reader is available for free from get.adobe.com/reader.

DISPLAYING THE TOOLBARS

Adobe Reader DC

In Adobe Reader DC, the Comment toolbar can be found by clicking 'Comment' in the menu on the right-hand side of the page (shown below).

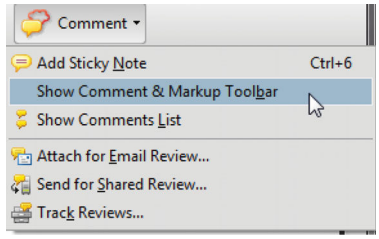


The toolbar shown below will then display along the top.



Acrobat Professional 7, 8, and 9

In Adobe Professional, the Comment toolbar can be found by clicking 'Comment(s)' in the top toolbar, and then clicking 'Show Comment & Markup Toolbar' (shown below).

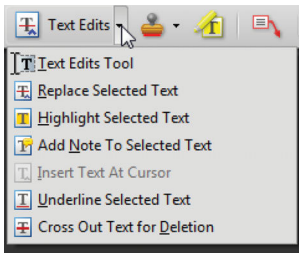


The toolbar shown below will then be displayed along the top.



USING TEXT EDITS AND COMMENTS IN ACROBAT

This is the quickest, simplest and easiest method both to make corrections, and for your corrections to be transferred and checked.



1. Click **Text Edits**
2. Select the text to be annotated or place your cursor at the insertion point and start typing.
3. Click the **Text Edits** drop down arrow and select the required action.

You can also right click on selected text for a range of commenting options, or add sticky notes.

SAVING COMMENTS

In order to save your comments and notes, you need to save the file (**File, Save**) when you close the document.

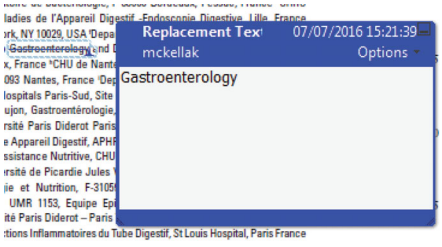
USING COMMENTING TOOLS IN ADOBE READER

All commenting tools are displayed in the toolbar. You cannot use text edits, however you can still use highlighter, sticky notes, and a variety of insert/replace text options.

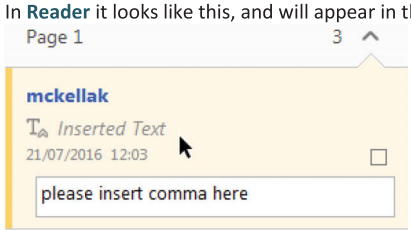


POP-UP NOTES

In both Reader and Acrobat, when you insert or edit text a pop-up box will appear. In **Acrobat** it looks like this:



In **Reader** it looks like this, and will appear in the right-hand pane:



DO NOT MAKE ANY EDITS DIRECTLY INTO THE TEXT, USE COMMENTING TOOLS ONLY.

Proximal Parent Vessel Tapering is Associated With Aneurysm at the Middle Cerebral Artery Bifurcation

Alexandra Lauric, PhD*
Kilian Greim-Kuczewski, MD*
Alexei Antonov*
Gabriel Dardik*
Jane K. Magida, MSc*
James E. Hippelheuser, BSc*
Kenichi Kono, MD‡
Adel M. Malek, MD, PhD*

*Department of Neurosurgery, Tufts Medical Center, Tufts University School of Medicine, Boston, Massachusetts; ‡Department of Neurosurgery, Showa University Fujigaoka Hospital, Kanagawa, Japan;

IRB approval: This research was approved by Tufts Health Sciences Campus Institutional Review Board. Patient consent was waived because of the retrospective nature of the study not impacting patient clinical care.

Correspondence:
Adel M. Malek, MD, PhD,
Department of Neurosurgery,
Tufts Medical Center,
800 Washington Street,
Boston, MA 02111.
E-mail: amalek@tuftsmedicalcenter.org

Received, September 27, 2017.
Accepted, March 27, 2018.

Copyright © 2018 by the
Congress of Neurological Surgeons

BACKGROUND: Cerebral aneurysm initiation and evolution have been linked to hemodynamic and morphological factors. Stenotic morphology upstream to a bifurcation can alter hemodynamic patterns and lead to destructive vessel wall remodeling and aneurysm initiation. The effect of more subtle proximal variations in vessel diameter on bifurcation aneurysm development has not been evaluated.

OBJECTIVE: To investigate whether vessel tapering is associated with aneurysmal presence at the middle cerebral artery (MCA) bifurcation.

METHODS: Bilateral catheter three-dimensional rotational angiographic datasets from 33 patients with unilateral unruptured MCA aneurysms and 44 datasets from healthy patients were analyzed. Equidistant cross-sectional cuts were generated along the MCA M1 segment with cross-sectional area measurement using edge-detection filtering. Relative tapering of the M1 segment was evaluated as the TaperingRatio. Computational fluid dynamics (CFD) simulations were performed on bilateral patient models and parametric MCAs of constant and tapered inflow vessel.

RESULTS: MCA leading to aneurysms had significantly lower TaperingRatio (0.88 ± 0.15) compared to contralateral (1.00 ± 0.16, $P = .002$) and healthy MCAs (1.00 ± 0.15, $P > .001$, area under the curve $= 0.73$), which showed little to no tapering. CFD simulations showed that vessel tapering leads to flow acceleration with higher wall shear stress (WSS) and WSS gradients at the bifurcation apex.

CONCLUSION: Aneurysmal but not contralateral or control MCA M1 segments demonstrate a previously undescribed progressive distal tapering phenomenon. This upstream vessel narrowing leads to flow acceleration that accentuates WSS and spatial gradients at the bifurcation apex, a pattern previously shown to favor aneurysm initiation and progression.

KEY WORDS: Intracranial aneurysms, Aneurysm formation, Vessel tapering, Hemodynamics

Neurosurgery 0:1–8, 2018 DOI:10.1093/neuros/nyy152 www.neurosurgery-online.com

Vessel morphology influences hemodynamic patterns and plays a role in the process of initiation, growth, and possible rupture of cerebral aneurysms.[1] Both hemodynamic[2] and morphological[3] parameters have been associated with aneurysm progression, and recent research proposed an interdependence between vessel morphology and the associated hemodynamics.[4] Endothelial cells have been shown to be highly responsive to the presence of high wall shear stress (WSS), particularly in the presence of positive WSS gradients (WSSG). This specific hemodynamic environment has been associated with destructive cellular responses and endothelial misalignment, leading to wall weakening over time.[5] Predisposing vessel morphologies[4,6] have been previously associated with aneurysm formation and presence.[7,8] Surgically altering the vessel morphology by either creating arterial bifurcations from native

ABBREVIATIONS: 3D, three-dimensional; **3DRA,** three-dimensional catheter-based cerebral angiograms; **ATA,** anterior temporal artery; **AUC,** area under the curve; **CFD,** computational fluid dynamics; **DistalCSA,** distal cross-sectional area; **ICA,** internal carotid artery; **MCA,** middle cerebral artery; **NarrowCSA,** narrowest cross-sectional area; **ProximalCSA,** proximal cross-sectional area; **ROC,** receiver operating characteristics curve; **VOP,** vascular optimality principle; **WSS,** wall shear stress; **WSSG,** WSS gradients

common carotid arteries,[5] or by therapeutic parent artery occlusions,[9] was shown to trigger changes in hemodynamic patterns and lead to de novo aneurysm formation. Recently, clinical studies showed that a marked decrease in the lumen caliber, as is the case for instance with stenotic vessels leading to cerebral bifurcations, results in distal hemodynamic elevation at the apex, and can create hemodynamic conditions predisposing to aneurysm origination.[10,11]

It has been previously suggested that the cerebral arterial vasculature follows the vascular optimality principle (VOP) that enforces minimization of energy loss across bifurcations and requires optimal caliber control between the vessels involved in the bifurcations.[12-14] Studies have shown, however, that aneurysmal bifurcations tend to deviate from VOP.[15] A large study on middle cerebral artery (MCA) bifurcations found that a third of aneurysmal bifurcations revealed a daughter branch larger than the parent, in absolute violation of the optimality.[15] These findings suggest a need for a better understanding of the bifurcation morphology and the conditions leading to aneurysm formation.

Here we investigate possible associations between tapering of the hosting vessel and aneurysm presence at the distal bifurcation. We hypothesize different degrees of tapering between vessels leading to aneurysms and control vessels. The analysis is focused on the M1 segment of the MCA and is performed bilaterally in patients harboring unilateral unruptured MCA bifurcation aneurysms, as well as in healthy controls.

METHODS

Patient Selection and Demographics

Consecutive high-resolution three-dimensional (3D) angiographic data of patients undergoing cerebral angiography between 2009 and 2012 were reviewed for this study. All studies of sufficient imaging quality to permit accurate segmentation and morphological analysis were included in the study. Consequently, a total of 33 bilateral datasets from patients with unilateral unruptured MCA aneurysms (Figures 1A and 1B) were included (28 females). In addition, 44 datasets from healthy patients with no aneurysms (Figure 1C) were available for analysis (24 females).

This research was approved by the Institutional Review Board. Patient consent was waived because of the retrospective nature of the study not impacting patient clinical care.

Cerebral Angiography and Data Processing

Three-dimensional catheter-based cerebral angiograms (3DRA) were obtained using a Siemens Artis (Malvern, Pennsylvania) calibrated biplane system, with volume reconstruction using the available Siemens Leonardo clinical software package, to yield a 3D volumetric dataset. Volumetric datasets, including aneurysm and parent vessel, were analyzed using Amira 5.3 (FEI, Hillsboro, Oregon) and Matlab R2017 (MathWorks, Natick, Massachusetts).

Morphological Feature Extraction

The skeleton (centerline) of the M1 segment of the MCA (Figure 2A) was generated using Amira (FEI) and exported to Matlab (MathWorks) to generate orthogonal cross-sections along the entire M1 segment (Figure 2B). Edge-detection filtering was applied to all cross-sections. Cross-sectional area of the M1 was evaluated from the edge-detection results (Figure 2C). In order to ensure that area measurements are a true reflection of the vessel morphology, the most proximal and most distal cross-sections along the M1 segment were considered just outside of the internal carotid artery (ICA) and MCA bifurcations area, respectively, approximately 1 M1 diameter away from the bifurcation apex. The following measurements were used for analysis: (1) the proximal cross-sectional area (ProximalCSA) of the M1 segment, measured 1 diameter from the ICA bifurcation, (2) the distal cross-sectional area (DistalCSA) as the area of the most distal plane cut closest to the MCA bifurcation measured 1 diameter from the MCA bifurcation, (3) the narrowest cross-sectional area (NarrowCSA) as the area of the most narrow plane cut, (4) the relative degree of stenosis (NarrowToProximalCSA) as the ratio of NarrowCSA and ProximalCSA, (5) the tapering of the M1 segment (TaperingRatio) defined as DistalCSA/ProximalCSA, as the ratio of DistalCSA and ProximalCSA, and (6) the proximal to distal distance (ProxToDistalDist) approximates the length of the M1 segment and is computed as the summation of the distance between consecutive plane cuts along the M1 parent vessel segment.

For some datasets, the anterior temporal artery (ATA) is clearly visible on the angiographic images and the 3D vessel segmentation. In these cases, the cross-sectional area was evaluated immediately before (Proximal ATA) and after (Distal ATA) the ATA (Figure 2C). These measurements were used to evaluate the effect of ATA presence on M1 tapering.

Statistical Analysis

JMP statistical software (Version 12.1.0, SAS Institute, Cary, North Carolina) was used to evaluate the performance of all parameters in discriminating between aneurysmal and control MCA datasets. Statistical significance was assumed for $P < .05$. All variables were tested independently using the student t-test analysis. Bilateral MCA analysis was performed using matched-pair analysis. Receiver operating characteristics curve (ROC) was performed and prediction accuracy was evaluated using the area under the curve (AUC) index. Optimal threshold values were determined using ROC statistics.

Parametric Models

In order to evaluate the effect of vessel tapering on the bifurcation hemodynamic environment, parametric models of the MCA bifurcation were constructed using SolidWorks (Concord, Massachusetts; Figure 3). Four models were created with an initial straight parent vessel having a length of 10 mm and a diameter of 2.6 mm, followed by a straight tapered segment having a length of 15 mm. Symmetrical daughter vessels (length of 10 mm and radius of 1.032 mm) were joined to the inflow vessel with an angle of 160°. The combination of the radii for the parent and daughter vessels follows the VOP.[12] The models were created with tapering ratios of 1.00 (not tapered), 0.86, 0.73, and 0.60 (Figure 3).

Patient-derived models were created for an aneurysmal MCA and the corresponding nonaneurysmal contralateral. The aneurysm was digitally removed by local Laplacian smoothing followed by aneurysm surface reconstruction in MeshLab version 1.3.1 (ISTI-CNR, Pisa, Italy). All models had a sufficiently long inflow vessel (several times the diameter

UNCORRECTED PROOF

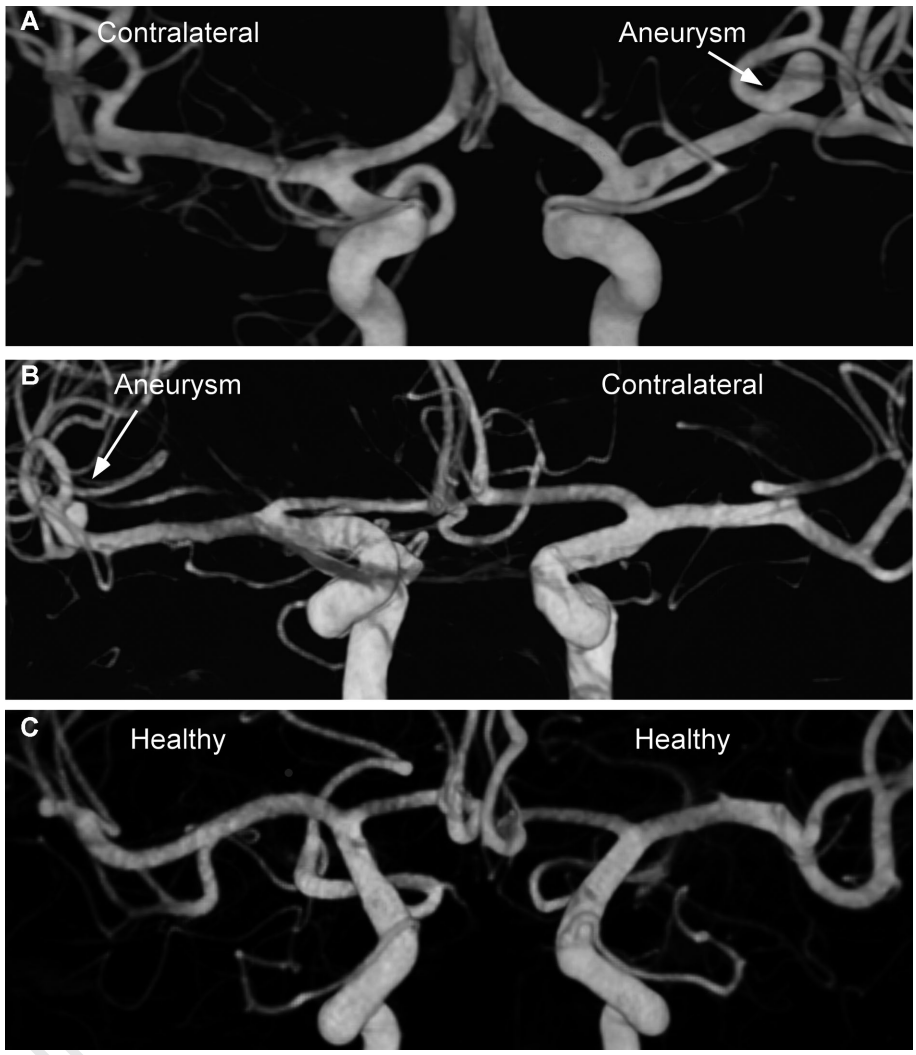


FIGURE 1. **A** *and* **B**, *Maximum intensity projection of bilateral 3DRA data for patients with unilateral MCA aneurysms.* **C**, *Maximum intensity projection of bilateral 3DRA data for a healthy control patient.*

of the parent vessel) proximal to the site of the aneurysm to ensure flow stabilization (Figure 4).

Computational Fluid Dynamics

CFD simulations were performed using Ansys Fluent 16.2 (Ansys Inc, Labanon, New Hampshire), by modeling laminar transient flow with a Carreau non-Newtonian profile to better approximate the viscosity and flow of blood.[16] For each model, the velocity magnitude was scaled to a proximal parent vessel WSS of approximately 1.5 Pa at the straight vessel inlet.[17] Pulsatile flow was applied at the inlet for 3 complete cardiac cycles to allow flow to develop adequately and the third cycle was used for analysis. Each cycle period was T = 1 s and had a time step of t = 0.002 s with the peak-systole at t = 0.16 s. At the outlets, gauge pressure was set to zero pascal.[18]

All postprocessing analysis was performed using EnSight 10.1 (Computational Engineering International, Apex, North Carolina). For each model, time-averaged WSS and spatial WSSG were analyzed along a longitudinal cut covering the apex of the bifurcation and extending downstream.

RESULTS

The M1 segment was evaluated on 33 MCA aneurysms compared against the 33 corresponding nonaneurysmal contralateral and 44 healthy MCAs.

In matched-pair analysis, M1 leading to aneurysmal MCA bifurcation had significantly smaller DistalCSA (4.77 ± 1.06 vs 5.33 ± 1.02 mm^2, $P = .0005$), lower NarrowToProximalCSA

COLOUR ONLINE, B&W IN PRINT

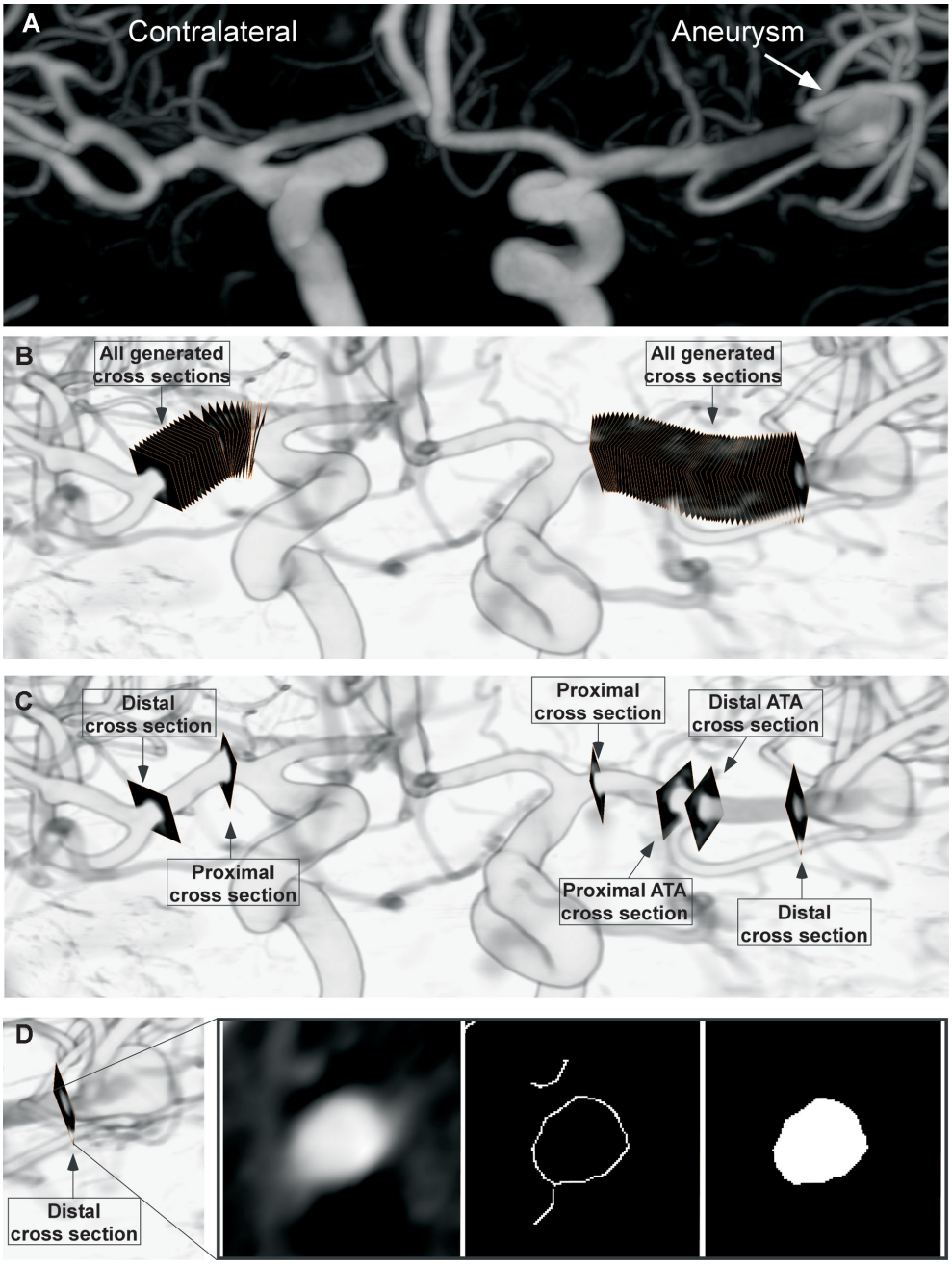


FIGURE 2. **A**, *Maximum intensity projection of bilateral 3DRA data for a patient with left MCA aneurysm and nonaneurysmal contralateral.* **B**, *Cross-sectional cuts are automatically generated along the M1 segments.* **C**, *The distal and proximal cross-sections are selected approximately 1 diameter from the bifurcations. In the presence of a visible anterior temporal artery (ATA), cross-sectional area is evaluated proximally and distally from the vessel.* **D**, *Edge-detection filter is applied on each cross-sectional cut plane. Cross-sectional area of the M1 is calculated based on the detected M1 edge.*

COLOUR ONLINE, B&W IN PRINT

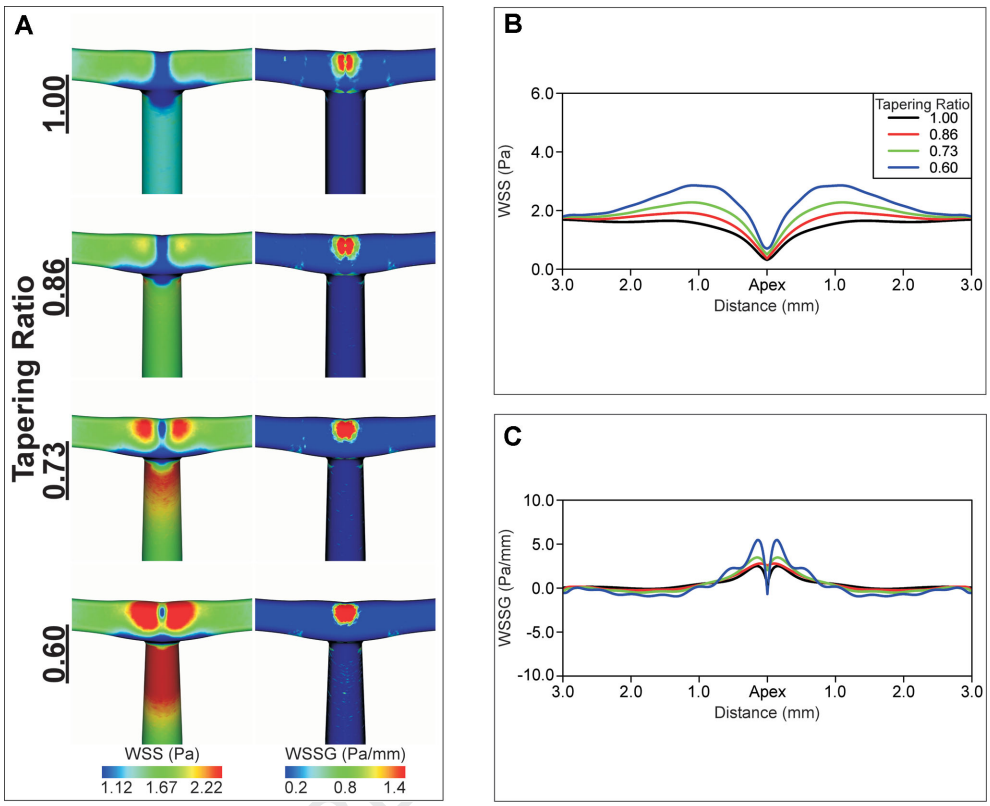


FIGURE 3. *CFD simulations on parametric models with constant and tapered inflow vessel.* **A**, *Four models are created with TaperingRatios of 1.00, 0.86, 0.73, and 0.60.* **B**, *WSS distributions at the apex show an increase of WSS with decreased TaperingRatio.* **C**, *WSSG distributions at the apex show an increase of positive WSSG magnitude and the area of high WSSG with decreased TaperingRatio.*

ratio (0.81 ± 0.11 vs 0.88 ± 0.09 mm^2, P = .01), and lower TaperingRatio (0.88 ± 0.15 vs 1.00 ± 0.16 mm^2, P = .002) compared to the contralateral M1 segment (Table 1). Smaller ratios suggest that MCA segments leading to aneurysms display greater vessel tapering progressing from proximal to distal, a phenomenon not observed in nonaneurysmal and healthy controls.

When comparing MCA aneurysms with healthy controls, there was no statistical difference between the ages of the 2 groups (Table 2). M1 leading to aneurysmal MCA bifurcation had significantly lower DistalCSA (4.77 ± 1.06 vs 5.33 ± 1.02 mm^2, P = .04), lower NarrowToProximal CSA ratio (0.81 ± 0.11 vs 0.89 ± 0.09 mm^2, P = .003), and lower TaperingRatio (0.88 ± 0.15 vs 1.00 ± 0.15 mm^2, P = .0007) compared to controls. TaperingRatio prediction accuracy as measured by area under the ROC was 0.73 (Table 2). An optimal threshold value of 0.92 was established for the TaperingRatio, with 88% specificity and 67% sensitivity.

There was no statistical difference between nonaneurysmal contralateral and healthy controls. It is interesting to note that all nonaneurysmal datasets (contralateral and healthy) had a mean TaperingRatio of 1 (1.00 ± 0.15) indicative of little to no tapering. Instead, in some cases of healthy controls the cross-sectional area of the M1 segment even increased slightly distally.

It should be noted that our use of cross-sectional area is more sensitive to diameter decrease compared to reporting the change in diameter. For instance, 0.88 TaperingRatio indicates a 0.12 decrease in CSA but only a 0.07 decrease in diameter (assuming a circular CSA). This allowed for the identification of subtle changes in vessel tapering.

There was no statistical difference between the lengths of M1 segments leading to MCA aneurysms compared to M1 segments leading to nonaneurysmal bifurcations. Thus, the difference in tapering has to do with the difference in DistalCSA and not with a longer segment.

Effect of ATA on Vessel Tapering

Out of 110 datasets, 39 (35%) had a visible ATA. Within the healthy group there were 20 samples (45%) with a visible ATA, compared with 13 samples (39%) with a visible ATA in

COLOUR ONLINE, B&W IN PRINT

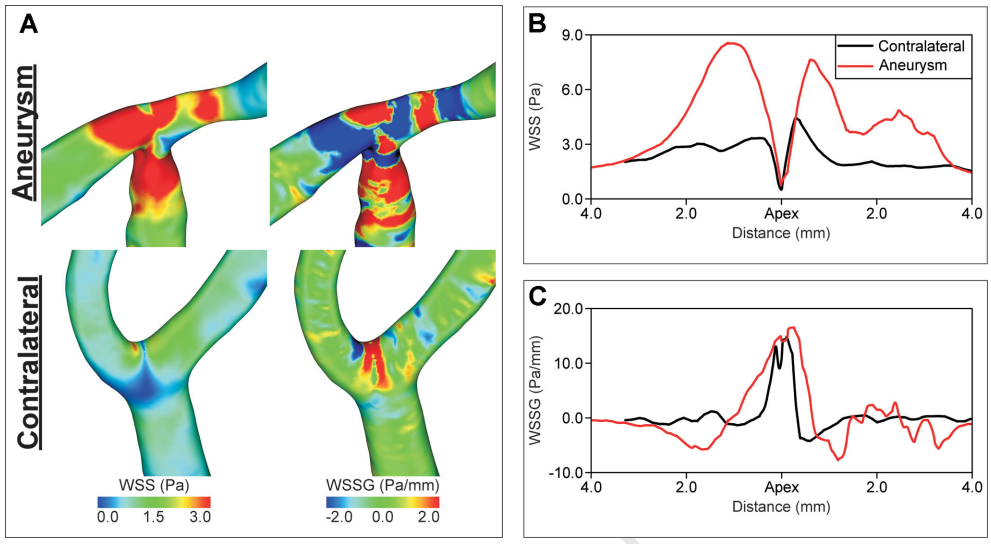


FIGURE 4. **A**, *CFD simulations on patient-derived models was performed on aneurysmal MCA (TaperingRatio 0.65) and the control contralateral (TaperingRatio 0.81). The aneurysm was removed before simulations.* **B**, *WSS distributions at the apex show high WSS on the aneurysmal side.* **C**, *WSSG distributions at the apex show larger area of positive WSSG on the aneurysmal side compared to control.*

TABLE 1. Matched Pair Statistical Analysis of MCA Parameters Between Aneurysmal Side and Corresponding Nonaneurysmal Contralateral

	Aneurysm (n = 33)	Contralateral (n = 33)	*P*-value
DistalCSA [mm^2]	4.77 ± 1.06	5.33 ± 1.02	.0005*
ProximalCSA [mm^2]	5.47 ± 1.11	5.41 ± 1.01	.64
NarrowCSA [mm^2]	4.40 ± 0.92	4.74 ± 0.88	.007*
NarrowToProximalCSA Ratio	0.81 ± 0.11	0.88 ± 0.09	.01*
TaperingRatio	0.88 ± 0.15	1.00 ± 0.16	.002*
ProxToDistalDist [mm]	15.66 ± 5.89	14.14 ± 7.07	.22

DistalCSA: distal cross-sectional plane cut of the M1 segment, closest to the MCA bifurcation; ProximalCSA: proximal cross-sectional plane cut of the M1 segment, closest to the ICA bifurcation; NarrowCSA: narrowest cross-sectional area of the M1 segment; NarrowToProximalCSA Ratio: the relative narrowing of the M1 segment; TaperingRatio: the tapering of the M1 segment defined as DistalCSA/ProximalCSA; and ProxToDistalDist: distance from the proximal to distal plane cuts that approximates M1 length. Shown are mean and standard deviation. *indicates statistical significance, which was assumed for $P < .05$.

TABLE 2. Univariate Statistical Analysis of MCA Parameters in Discriminating Between Aneurysmal and Healthy Samples

	Aneurysm (n = 33)	Healthy (n = 44)	*P*-value	AUC
DistalCSA [mm^2]	4.77 ± 1.06	5.34 ± 1.02	.04*	0.63
ProximalCSA [mm^2]	5.47 ± 1.11	5.30 ± 1.02	.49	
NarrowCSA [mm^2]	4.40 ± 0.92	4.72 ± 1.07	.17	
NarrowToProximalCSA	0.81 ± 0.11	0.89 ± 0.09	.003*	0.68
TaperingRatio	0.88 ± 0.15	1.00 ± 0.15	.0007*	0.73
ProxToDistalDist[mm]	15.66 ± 5.89	14.80 ± 5.35	.22	
Age [yr]	57 ± 13.76	52.21 ± 12.75	.08	

DistalCSA: distal cross-sectional plane cut of the M1 segment, closest to the MCA bifurcation; ProximalCSA: proximal cross-sectional plane cut of the M1 segment, closest to the ICA bifurcation; NarrowCSA: narrowest cross-sectional area of the M1 segment; NarrowToProximalCSA Ratio: the relative narrowing of the M1 segment; TaperingRatio: the tapering of the M1 segment defined as DistalCSA/ProximalCSA; ProxToDistalDist: distance from the proximal to distal plane cuts that approximates M1 length. Shown are mean and standard deviation. *indicates statistical significance, which was assumed for $P < .05$. Area under the ROC curve (AUC) was evaluated for statistically significant parameters.

Q3

the aneurysmal group. Only 6 contralateral samples presented with a visible ATA. There was no significant difference between aneurysmal M1 segments and healthy controls regarding the presence of ATA.

For those M1 segments with visible ATA (13 aneurysmal/20 healthy), the segment tapering was evaluated proximally from the ICA bifurcation to the ATA (as Proximal ATA/ProximalCSA) and distally from the ATA to the MCA bifurcation (as DistalCSA/DistalATA). On the proximal segments, there was no statistical difference in tapering between aneurysms and controls. However, on the distal segment, from the ATA to MCA bifurcation, M1 segments leading to aneurysms had statistically significant tapering compared to controls (0.93 ± 0.11 vs 1.02 ± 0.11, $P = .03$).

UNCORRECTED

In addition, analysis performed exclusively on the remaining M1 segments without ATA showed that aneurysmal M1 had significant tapering compared to controls (0.89 ± 0.16 vs 1.02 ± 0.15, $P = .01$). Aneurysmal M1 segments showed tapering regardless of ATA presence.

Finally, we repeated the analysis on the whole dataset (33 aneurysms/44 healthy) and considered tapering as either the tapering of the entire M1 segment if there was no ATA, or as the tapering of the distant segment from ATA to MCA bifurcation if the ATA vessel was present. As expected, M1 leading to aneurysms showed significant tapering compared to controls (0.91 ± 0.14 vs 1.02 ± 0.13, $P = .0009$, AUC = 0.70), validating our overall results.

Computational Fluid Dynamics

CFD analysis on parametric MCA models showed that tapering induced an increase in absolute magnitude of WSS and WSSG at the bifurcation apex (Figure 3).

Maximum WSS at apex increased progressively with tapering from 1.65 Pa in the model with not tapering (TaperingRatio 1.00) to 2.85 Pa in the model with the highest degree of tapering (TaperingRatio 0.60) representing 72% WSS increase at maximum values (Figure 3B).

Similarly maximum positive WSSG at apex increased from 2.50 Pa/mm in the model with not tapering (TaperingRatio 1.00) to 5.54 Pa/mm in the model with the highest degree of tapering (TaperingRatio 0.60) representing 121% WSSG increase at maximum values (Figure 3C).

CFD analysis on bilateral MCA bifurcations of a patient harboring unilateral MCA aneurysm (Figure 4A), showed that the highly tapered M1 leading to MCA aneurysms (TaperingRatio 0.65) had high WSS (maximum value at the apex 8.55 Pa) and high WSSG (maximum value at the apex 14.93 Pa/mm). In contrast the maximum WSS at the contralateral apex was 4.4 Pa (Figure 4B). The absolute peak values for WSSG are somewhat similar for contralateral and aneurysmal side, however should be noted that the high positive WSSG covers a much wider apex area on the aneurysmal side (Figure 4C).

DISCUSSION

To the best of our knowledge, we have described for the first time the presence of proximal vessel smooth tapering in patients harboring unruptured aneurysms at the middle cerebral artery. This phenomenon seems to be strongly associated with aneurysm presence since it was not observed in contralateral nonaneurysmal bifurcations.

Previously, dramatic alterations to vessel morphology were shown to trigger hemodynamic changes associated with cerebral aneurysm initiation, such as high WSS and high positive WSSG. De novo aneurysm formation was previously reported following therapeutic carotid artery occlusions.[9] Unilateral or bilateral common carotid artery ligation in animal studies were shown to lead to endothelial cells remodeling consistent with aneurysm initiation due to flow increase in the modified vessel, without any other known predisposing factors.[19,20] Vessel stenosis, which modifies the original tubular structure, was previously associated with de novo aneurysm formation.[10,11,21]

However, the aneurysmal MCAs studied here showed neither stenosis nor morphological alterations, presenting instead with smooth vessel tapering leading to flow acceleration in the bifurcation area. Because our analysis was performed on cross-sectional area instead of vessel diameter, it was more sensitive to subtle changes and it showed that aneurysmal MCAs had statistically significant tapering compared to healthy controls, but also with the corresponding nonaneurysmal contralaterals MCA segments. In fact, whereas M1 segments associated with MCA aneurysms had a mean tapering ratio of 0.88, both healthy and contralateral M1 segments had a mean tapering ratio of 1.00 (1.00 ± 0.15) meaning their M1 segments maintained a constant cross-sectional area. In the presence of a prominent ATA, the vessel tapering was seen to occur distally from the origin of this vessel, but did not impact the overall findings and analysis.

Kono et al[10,11] showed that proximal stenosis triggers high WSS and high positive WSSG at the bifurcation apex. These conditions have been previously associated with destructive endothelial remodeling consistent with aneurysmal initiation.[5] Here we show that vessel tapering also increases the WSS and WSSG at the bifurcation apex, both in parametric and patient models. These hemodynamic conditions at the bifurcation, previously associated with aneurysm formation at bifurcations,[1] are one possible explanation for aneurysm initiation in tapered bifurcations.

Although the flow acceleration from the gentle tapering could explain the aneurysm genesis, other possibility is that the vessel narrowing is just a reflection of poor local vessel caliber control, which leads to failure of the VOP at the bifurcation and could explain aneurysm presence at these locations. Cerebral arterial network is believed to obey VOP. According to the principle, the radius of the parent vessel (r_0) dictates the radii of its daughter branches (r_1, r_2,..., r_i) according to the formula $r_0^n = r_1^n + r_2^n + \ldots + r_i^n$, in which n is the junction exponent with a theoretical value of approximately 3 in human cerebral arterial bifurcations.[12,14,22] It was previously shown using 3DRA data that normal, but not aneurysmal, MCA bifurcation follow VOP. Although the formula enforces daughter vessels smaller than the parent vessel, it was shown that more than one third of MCA bifurcations harboring aneurysms have daughter vessels wider than their parent vessels, in clear violation of the VOP.[15]

Our findings raise the possibility that the optimality failure previously reported in MCA bifurcations[15] could be due to parent vessel tapering and not necessary a widening of the proximal M2 segment as we initially hypothesized. The possible connection between VOP and vessel tapering as well as the clinical implications needs to be further explored in future studies. Future research will be needed to determine whether this phenomenon is location specific or of a more global significance in aneurysm development.

UNCORRECTED PROOF

Limitations

This research showed that quantitative analysis of diameter variations along the M1 segment of the MCA can be used to discriminate between aneurysmal and nonaneurysmal MCA bifurcations. As it is the case with similar retrospective research, the association between vessel narrowing and aneurysm presence suggests a correlation, but does not imply causation. The conclusions of this study will require validation by further research.

An additional question is whether the tapering effect presented here could represent an imaging artifact owing to flow effects related to aneurysm presence. We believe this is unlikely given the relatively small sizes of the aneurysms in this population (5.15 ± 2.02 mm). In addition, some controls also displayed tapering, although as a group nonaneurysmal controls had significantly less tapering compared to vessels leading to aneurysms.

CONCLUSION

We have described a novel phenomenon of proximal vessel tapering in unruptured aneurysm bearing bifurcations. Whereas the relative tapering of the M1 segment of the MCA is indicative of aneurysm presence, healthy and nonaneurysmal contralateral show no tapering. This upstream vessel narrowing leads to flow acceleration that accentuates WSS and spatial gradients at the bifurcation apex, a pattern previously shown to favor aneurysm initiation and progression. Vessel tapering seems to be a local phenomenon present in aneurysmal bifurcations, but not in their nonaneurysmal contralaterals, a finding with potential implications and uses in screening of cerebral bifurcations morphologically predisposed to aneurysm formation.

Disclosures

The senior author (Dr Malek) has received unrestricted research funding by Stryker Neurovascular for research that is unrelated to the submitted work. The authors have no personal, financial, or institutional interest in any of the drugs, materials, or devices described in this article.

REFERENCES

1. Sforza DM, Putman CM, Cebral JR. Hemodynamics of cerebral aneurysms. *Annu. Rev. Fluid Mech*. 2009;41(1):91-107.
2. Xiang J, Natarajan SK, Tremmel M, et al. Hemodynamic-morphologic discriminants for intracranial aneurysm rupture. *Stroke*. 2011;42(1):144-152.
3. Baharoglu MI, Lauric A, Gao B-L, Malek AM. Identification of a dichotomy in morphological predictors of rupture status between sidewall- and bifurcation-type intracranial aneurysms. *J Neurosurg*. 2012;116(4):871-881.
4. Tütüncü F, Schimansky S, Baharoglu MI, et al. Widening of the basilar bifurcation angle: association with presence of intracranial aneurysm, age, and female sex. *J Neurosurg*. 2014;121(6):1401-1410.
5. Meng H, Swartz DD, Wang Z, et al. A model system for mapping vascular responses to complex hemodynamics at arterial bifurcations in vivo. *Neurosurgery*. 2006;59(5):1094-1101.
6. Baharoglu MI, Lauric A, Safain MG, Hippelheuser J, Wu C, Malek AM. Widening and high inclination of the middle cerebral artery bifurcation are associated with presence of aneurysms. *Stroke*. 2014;45(9):2649-2655.
7. Piccinelli M, Bacigaluppi S, Boccardi E, et al. Geometry of the internal carotid artery and recurrent patterns in location, orientation, and rupture status of lateral aneurysms: an image-based computational study. *Neurosurgery*. 2011;68(5):1270-1285.
8. Lauric A, Safain MG, Hippelheuser J, Malek AM. High curvature of the internal carotid artery is associated with the presence of intracranial aneurysms. *J Neurointerv Surg*. 2014;6(10):733-739.
9. Arambepola PK, McEvoy SD, Bulsara KR. De novo aneurysm formation after carotid artery occlusion for cerebral aneurysms. *Skull Base*. 2010;20(6):405-408.
10. Kono K, Fujimoto T, Terada T. Proximal stenosis may induce initiation of cerebral aneurysms by increasing wall shear stress and wall shear stress gradient. *Int J Numer Method Biomed Eng*. 2014;30(10):942-950.
11. Kono K, Masuo O, Nakao N, Meng H. De novo cerebral aneurysm formation associated with proximal stenosis. *Neurosurgery*. 2013;73(6):E1080-E1090.
12. Rossitti S, Lofgren J. Vascular dimensions of the cerebral arteries follow the principle of minimum work. *Stroke*. 1993;24(3):371-377.
13. Rossitti S, Lofgren J. Optimality principles and flow orderliness at the branching points of cerebral arteries. *Stroke*. 1993;24(7):1029-1032.
14. Ingebrigtsen T, Morgan MK, Faulder K, Ingebrigtsen L, Sparr T, Schirmer H. Bifurcation geometry and the presence of cerebral artery aneurysms. *J Neurosurg*. 2004;101(1):108-113.
15. Baharoglu MI, Lauric A, Wu C, Hippelheuser J, Malek AM. Deviation from optimal vascular caliber control at middle cerebral artery bifurcations harboring aneurysms. *J Biomech*. 2014;47(13):3318-3324.
16. Schirmer CM, Malek AM. Wall shear stress gradient analysis within an idealized stenosis using non-Newtonian flow. *Neurosurgery*. 2007;61(4):853-864.
17. Malek AM, Alper SL, Izumo S. Hemodynamic shear stress and its role in atherosclerosis. *JAMA*. 1999;282(21):2035-2042.
18. Bowker TJ, Watton PN, Summers PE, Byrne JV, Ventikos Y. Rest versus exercise hemodynamics for middle cerebral artery aneurysms: a computational study. *Am J Neuroradiol*. 2010;31(2):317-323.
19. Gao L, Hoi Y, Swartz DD, Kolega J, Siddiqui A, Meng H. Nascent aneurysm formation at the basilar terminus induced by hemodynamics. *Stroke*. 2008;39(7):2085-2090.
20. Metaxa E, Tremmel M, Natarajan SK, et al. Characterization of critical hemodynamics contributing to aneurysmal remodeling at the basilar terminus in a rabbit model. *Stroke*. 2010;41(8):1774-1782.
21. Samano A, Ishikawa T, Moroi J, Yamashita S, Suzuki A, Yasui N. Ruptured de novo posterior communicating artery aneurysm associated with arteriosclerotic stenosis of the internal carotid artery at the supraclinoid portion. *Surg Neurol*. 2011;23(2):35.
22. Rosen R. *Optimality Principle in Biology*.London: Butterworths; 1967.

UNCORRECTED PROOF